Subsynoptic-Scale Kinetic Energy Balance in the Storm Area[1,2]

ERNEST C. KUNG AND TED L. TSUI[3]

Department of Atmospheric Science, University of Missouri-Columbia, Columbia, Mo. 65201

(Manuscript received 25 July 1974, in revised form 13 November 1974)

ABSTRACT

The balance of kinetic energy under severe storm conditions is investigated with a subsynoptic-scale upper-air network. The general shape of vertical profiles of the kinetic energy generation and dissipation is very similar to that observed in well-developed major cyclones. The overall average magnitude of the observed energy transformations in the severe storm area is comparable to that of major synoptic-scale cyclones, but for a given storm the magnitude of energy transformations may vary widely depending on the existence and strength of mesoconvective systems in the area.

The balance of kinetic energy is also studied for the transient disturbances detected with the subsynoptic-scale upper-air network. Energetics features for those disturbances are depicted and discussed. The mid and lower troposphere appear to be the major source region of eddy kinetic energy.

1. Introduction

In the search for a comprehensive understanding of the general circulation, one major concern is the energetics properties of large to small scales of motions in the system. The energetics study of the subsynoptic scale concerns the processes of the scale range between the grid and individual mesoscale systems, particularly in the immediate vicinity of the grid scale. The "subsynoptic" scale as used here thus designates the range from about 100 km up to the grid scale. Despite its importance, very little information is available at present concerning the energetics of this scale range.

With special upper-air observations by the National Severe Storms Laboratory (NSSL) of the National Oceanic and Atmospheric Administration during thunderstorm periods in 1966 and 1967, a series of exploratory studies of subsynoptic-scale energetics has been performed as one phase of our energetics study of the general circulation (Behrens, 1972; Kung and Behrens, 1974; McInnis, 1970; McInnis and Kung, 1972; Wrigley, 1973). Among those studies, reports by McInnis (1970) and McInnis and Kung (1972) dealt with the evaluation of energy variables involved in the kinetic energy equation.

The large-scale motions are quasi-horizontal. The subsynoptic-scale motions are also quasi-horizontal, and to a certain degree the methodology of large-scale energetics for an estimate of energy parameters may be extended to this scale range by utilizing upper-air data from closely located network stations. Despite technical difficulties involved in the use of the dense upper-air network data during thunderstorm periods, we were able to form some qualitative discussions on transformations of kinetic energy with the NSSL data of the subsynoptic-scale network (McInnis, 1970; McInnis and Kung, 1972). Since then there have been significant improvements in our design of the numerical analysis scheme for kinematic estimates of the vertical motion field as well as for the analysis of the general meteorological fields with the upper-air network data (Kung, 1972, 1973). This allowed us the opportunity to analyze the subsynoptic-scale network data with more freedom in examination of energy parameters, and with more confidence in the presentation of the energy budget.

In this study the kinetic energy balance in the general flow and the kinetic energy balance in the observed spatial disturbances are evaluated and discussed with the same NSSL data. We would like to emphasize here that we are not trying to describe individual mesoscale convective systems, but rather we are attempting to observe the energy transformations under severe storm conditions with the subsynoptic-scale upper-air network in the context of the large-scale energetics.

2. Upper-air data and analysis of meteorological fields

Aerological soundings were made by NSSL in April, May and June of 1966 and 1967 during periods of

[1] Research supported by the National and International Programs, Office for Climate Dynamics, National Science Foundation.

[2] Contribution from the Missouri Agricultural Experiment Station, Journal Series Number 7058.

[3] Present affiliation: Department of Geosciences, North Carolina State University, Raleigh.

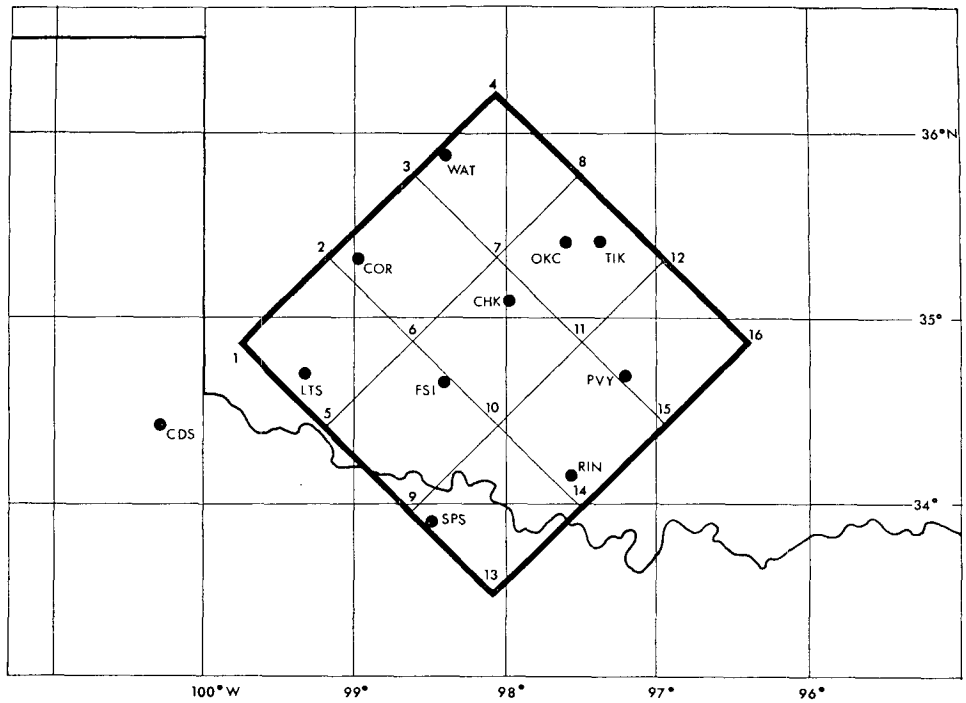

FIG. 1. NSSL 1966–67 upper-air network and analysis grids. Grids are numbered from 1 to 16.

thunderstorms, using a special upper-air network of 11 stations located principally in southwestern Oklahoma. As shown in Fig. 1, the network includes Fort Sill (FSI), Altus Air Force Base (LTS), Ringling (RIN), Chickasha (CHK), Tinker Air Force Base (TIK), Fauls Valley (PVY), Cordell (COR), Watonga (WAT) and Oklahoma City (OKC), Oklahoma, and Wichita Falls (SPS) and Childress Air Force Base (CDS), Texas. The network was activated prior to expected storms, and an interval of ~90 min was maintained between simultaneous releases of radiosonde balloons at all stations until major convective activities had ceased.

With an average separation of about 85 km between stations, the observation network had a much higher density than operational upper-air networks. Meteorological parameters were transmitted at a vertical interval of approximately 150 m during the ascent. The balloon position during ascent was recorded. For consistency the same NSSL storm data edited and used by McInnis (1970) and McInnis and Kung (1972) are utilized. Those include soundings during nine storm periods as identified by the date of initial observations: 4/22/66, 5/20/66, 5/31/66, 6/08/66, 5/20/67, 5/28/67, 5/30/67, 6/08/67, 6/10/67. It should be noted here that though the soundings were taken during the storm periods, the balloons released during those periods did not penetrate into strong individual convective cells. Thus the data may be viewed as representative of the environment of severe local storms observed at subsynoptic scale. Reference may be made to McInnis (1970) for details of the data editing and the general description of synoptic patterns during those storm periods. Utilizing those edited data, meteorological parameters were interpolated vertically for individual soundings as quadratic functions of the pressure level at every 20 mb interval from 960 to 100 mb. The pressure values at the surface were retained (968 mb was taken as the average surface pressure throughout this study). Those vertically interpolated data and surface data constitute the input data for the energetics analysis in this study.

As the basic requirement in estimating energetics variables in a space-time domain, the space variation of meteorological variables must be analyzed with the upper-air data. A diamond grid system with grid spacing of ~73 km is designed as shown in Fig. 1 to cover the network area. With observed upper-air data at recorded balloon positions on defined isobaric surfaces, basic meteorological parameters are estimated on grid points 1 through 16 as described in this section. The boundary of the area as defined by grid points 1, 2, 3, 4, 8, 12, 16, 15, 14, 13, 9, 5 is also the boundary along which line integrals are to be obtained for the estimate of the flux divergence of energy in the area.

The kinematic estimate of the vertical p-velocity $\omega = dp/dt$ is important in objective energy diagnosis as it is based on no assumptions about the nature of the circulation except the hydrostatic relationship. Kung (1972, 1973) designed an optimized computation scheme under the verified assumption that the vertical profile of ω should converge to a near-zero value at the top

of the atmosphere without being so forced when a sensitive balance between the analysis scheme and data disposition is achieved. The analysis scheme utilized in this study is a direct modification of Kung's (1973) scheme for the synoptic-scale network data to suit the subsynoptic-scale network data. The analysis scheme incorporates 15 degrees of optimization, and up to 15 alternative estimates of divergence and thus up to 15 alternative ω profiles are estimated at each grid.

Two basic degrees of optimization are provided by the estimates of divergence through the use of quadratic and plane surface approximations of the wind field at the grid points and stations with the observed winds at reported balloon positions. This step also gives interpolated winds at grid points and station locations. By re-approximating the quadratic and plane surfaces at grids and stations through addition of interpolated winds at grids and stations to observed winds at balloon positions, we obtained two additional degrees of optimization. We have two other degrees of optimization by re-approximating the quadratic and plane surfaces with the interpolated winds at grids and stations but without employing the original observation. A total of six alternative profiles of divergence estimates are thus obtained. Those six alternative estimates are then utilized to yield six additional alternatives through the use of the eigenvector method in terms of principal components analysis (Stidd, 1967) assuming that the divergence is a function of the three-dimensional location in the space. After computing 12 alternative ω profiles from 12 alternative divergence estimates, the selection process as described by Kung (1973) is applied to select the best profiles of ω and divergence at grids and stations. Further optimizations 13 through 15 are obtained through horizontal smoothing of divergence by algebraic average, plane surface approximation and quadratic surface approximation with those selected divergence values at neighboring grid points and stations. Final selection of ω (see Kung, 1973) will then be completed.

To vertically integrate divergence to obtain an ω profile, the ω value at surface should be specified to represent the terrain effect at subsynoptic scale. This lower boundary condition is approximated by

$$\omega_{\text{sfc}} = \mathbf{V}_{\text{sfc}} \cdot \nabla p_{\text{sfc}}, \tag{1}$$

where $\mathbf{V}$ is the vector of the horizontal wind, p the pressure, and ∇ the horizontal del operator. The subscript sfc denotes the surface value. Throughout the analysis, $|\omega_{\text{sfc}}|$ was about 0.5 μb s^{-1}, but the subsynoptic scale ω in the mid troposphere usually reaches between 10 and 20 μb s^{-1} during the storm periods. Thus the surface value of ω is rather insignificant.

Since the ω is estimated with subsynoptic-scale network data during the storm period, the trend of convergence of the ω profile at the top of the atmosphere

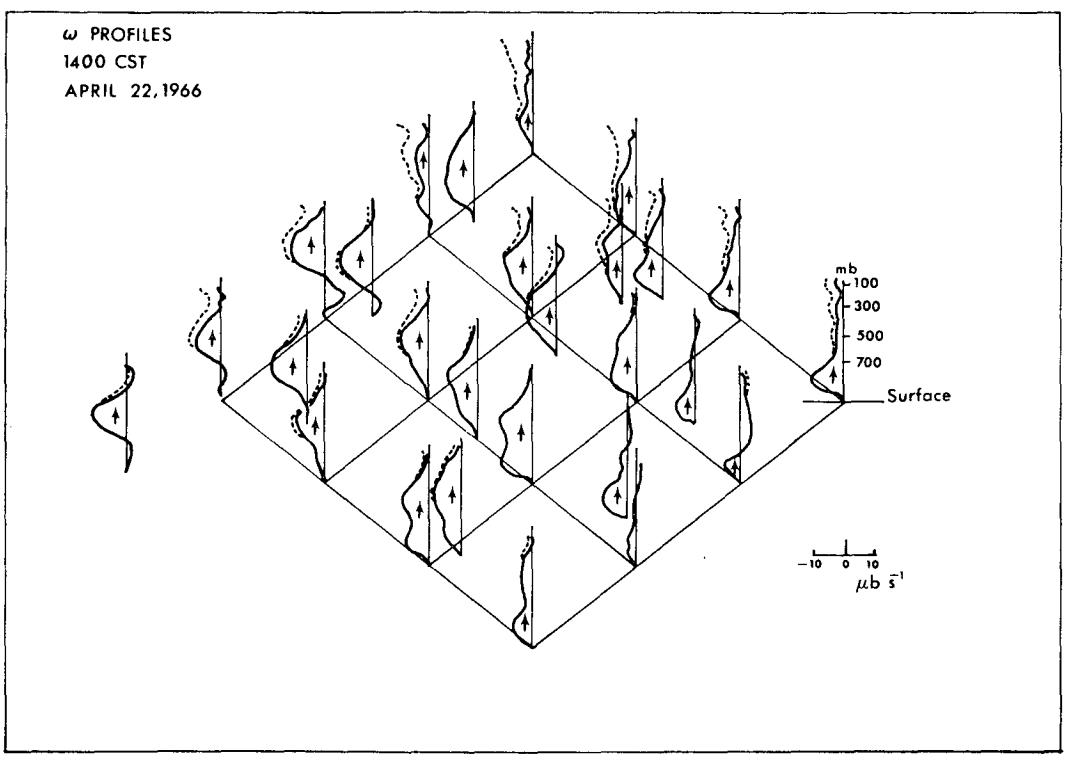

FIG. 2. Distribution of ω profiles at observation stations and analysis grids at 1400 CST 22 April 1966. Dotted lines are profiles before correction.

is not as uniform as in the case of the synoptic-scale network even with the optimized analysis scheme. After the selection of the ω profile, O'Brien's (1970) quadratic correction scheme is applied to the selected ω profiles at grids and stations with an assumed value of $\omega=0$ at the 10-mb level. Fig. 2 illustrates an arbitrary example of the vertical motion field at 1400 CST 22 April 1966 in terms of the ω profile before and after application of O'Brien's correction scheme. Considering the scale and technical difficulties involved in the use of subsynoptic-scale data, the quality of the obtained ω profiles seem to indicate their usefulness in further energetics analysis. A note may be in order here concerning the application of O'Brien's correction scheme to the selected ω profile. While O'Brien's scheme is recognized to be a workable correction scheme to force convergence of the ω profile at the top of the atmosphere, it is important to obtain an ω profile that needs a minimum of the correction before its application to ensure the quality of the vertical motion field obtained. In our scheme the correction scheme is used for the purpose of smoothing the field rather than forcing convergence at the top.

After the ω profile is selected at a grid point, the original polynomial surface configuration which has produced the selected divergence field is utilized to interpolate standard meteorological parameters at each grid point from the observed values. Those grid values of meteorological parameters, including those of ω, horizontal wind components, temperature and geopotential height, are utilized for evaluation of energy variables.

3. Budget equations and evaluation of energy variables

By taking the scalar product of the horizontal wind vector $\mathbf{V}$ and the equation of horizontal motion, and applying the equation of mass continuity, the kinetic energy equation may be written as

$$\frac{\partial k}{\partial t}=-\nabla\cdot\mathbf{V}k-\frac{\partial \omega k}{\partial p}-\mathbf{V}\cdot\nabla\phi-E, \tag{2}$$

where ϕ is the geopotential, E the dissipation and t the time. The kinetic energy per unit mass is

$$k=\tfrac{1}{2}(u^2+v^2), \tag{3}$$

where u and v are the eastward and northward wind components.

The mean value of a dummy variable X over the analysis area A along an isobaric surface may be defined by

$$[X]=\frac{1}{A}\int_A X\,dA, \tag{4}$$

and the kinetic energy equation (2) may be rewritten to express the kinetic energy balance of the atmospheric flow in the area of analysis:

$$\left[\frac{\partial k}{\partial t}\right]=-[\nabla\cdot\mathbf{V}k]-\left[\frac{\partial \omega k}{\partial p}\right]-[\mathbf{V}\cdot\nabla\phi]-[E]. \tag{5}$$

For the analysis of upper-air network data from a limited region, a convenient way to describe the spatial disturbance is to partition a variable into area mean and perturbation from the area mean. With the area mean defined by Eq. (4), a dummy variable may be expressed as

$$X=[X]+X^*, \tag{6}$$

where the perturbation from the mean X^* may be regarded as the space eddy. The eddy kinetic energy per unit mass may be defined as

$$k_e=\tfrac{1}{2}(u^{*2}+v^{*2}). \tag{7}$$

We may substitute dependent variables in the equation of motion with a respective sum of area mean and eddy quantities, and then apply the area-mean operator of Eq. (4). We then take the scalar product of the resultant equation and the area-mean horizontal wind vector to obtain the kinetic energy equation of the area-mean flow. By subtracting this kinetic energy equation of the area-mean flow from Eq. (5), we may obtain the eddy kinetic energy equation for the area:

$$\left[\frac{\partial k_e}{\partial t}\right]=-[\nabla\cdot\mathbf{V}k_e]-\left[\frac{\partial \omega k_e}{\partial p}\right]-\left\{[u^*\omega^*]\frac{\partial[u]}{\partial p}+[v^*\omega^*]\frac{\partial[v]}{\partial p}\right\}-[\mathbf{V}^*\cdot\nabla\phi^*]-[E^*]. \tag{8}$$

Reference may be made to Kung and Merritt (1974) and Kung (1975) with regard to the formulation of the eddy kinetic energy equation (8).

In an objective energy analysis, the utility of computations depends very much upon the nature of the data input into the budget equations. By applying Eq. (5) to the NSSL data, we obtain the balance of kinetic energy of the atmospheric flow observed with a subsynoptic-scale upper-air network. By applying Eq. (8) to the same data we observe the balance of kinetic energy in the space disturbances detected by the subsynoptic-scale network stations. We may regard Eq. (5) as the kinetic energy equation of the general flow, while Eq. (8) is the eddy kinetic energy equation for disturbances. It should be noted that the balance of eddy kinetic energy as represented in Eq. (8) is a component of the subsynoptic-scale kinetic energy balance as described in Eq. (5).

As used here $[\partial k/\partial t]$ and $[\partial k_e/\partial t]$ are the local time changes of the kinetic energy in the general flow and the eddies, $-[\nabla\cdot\mathbf{V}k]$ and $-[\nabla\cdot\mathbf{V}k_e]$ the horizontal

flux convergences or horizontal transports of kinetic energy, $-[\partial\omega k/\partial p]$ and $-[\partial\omega k_e/\partial p]$ the vertical flux convergences or vertical transports, $-[\mathbf{V}\cdot\nabla\phi]$ and $-[\mathbf{V}^*\cdot\nabla\phi^*]$ the cross-isobaric generations, and $[E]$ and $[E^*]$ the dissipations. The term

$$C=-\left\{[u^*\omega^*]\frac{\partial[u]}{\partial p}+[v^*\omega^*]\frac{\partial[v]}{\partial p}\right\} \tag{9}$$

is the energy conversion from the area-mean kinetic energy to eddy kinetic energy. Whereas $-[\nabla\cdot\mathbf{V}k]$, $-[\nabla\cdot\mathbf{V}k_e]$, $-[\partial\omega k/\partial p]$ and $-[\partial\omega k_e/\partial p]$ represent external sources of kinetic energy imported to the defined mass of the atmosphere over the region, $-[\mathbf{V}\cdot\nabla\phi]$, $-[\mathbf{V}^*\cdot\nabla\phi^*]$, and C may be considered as internal sources of kinetic energy.

The cross-isobaric generations $-[\mathbf{V}\cdot\nabla\phi]$ and $-[\mathbf{V}^*\cdot\nabla\phi^*]$ measure the adiabatic generation of kinetic energy due to ageostrophic acceleration of the flow which is the supply of kinetic energy from the reservoir of the available potential energy. As shown by Kung and Merritt (1974), the generation term of disturbances may be related to three eddy energy source terms:

$$-[\mathbf{V}^*\cdot\nabla\phi^*]=-[\nabla\cdot\mathbf{V}^*\phi^*]-\left[\frac{\partial\omega^*\phi^*}{\partial p}\right]-[\omega^*\alpha^*], \tag{10}$$

where $-[\omega^*\alpha^*]$ is the eddy conversion, and $-[\nabla\cdot\mathbf{V}^*\phi^*]$ and $-[\partial\omega^*\phi^*/\partial p]$ are respectively the eddy flux convergences of potential energy in the horizontal and vertical.

Energy variables involved in balance equations (5) and (8) and source terms in Eq. (10) are evaluated with the meteorological parameters obtained at the grid points as described in the preceding section. $-[\nabla\cdot\mathbf{V}k]$, $-[\nabla\cdot\mathbf{V}k_e]$ and $-[\nabla\cdot\mathbf{V}^*\phi^*]$ are computed with line integrals along the boundary of the defined area; other terms except $-[\mathbf{V}^*\cdot\nabla\phi^*]$, $[E]$ and $[E^*]$ are computed directly with the grid point values. Then $-[\mathbf{V}^*\cdot\nabla\phi^*]$ is obtained as the summation of the three terms on the right-hand side of (10), and $[E]$ and $[E^*]$ as the residual terms to balance (5) and (8). Direct computation of $-[\mathbf{V}\cdot\nabla\phi]$ is known for its difficulty for various reasons under various circumstances. However, as discussed by Kung and Smith (1974), a properly designed scheme of analysis can make a reliable estimate of this term with synoptic-scale network data. For a subsynoptic-scale network of this size, this term is more difficult to estimate. Yet McInnis and Kung (1972) have shown that meaningful results can still be obtained with the NSSL data, and the results in this paper with an improved scheme clearly demonstrate the validity of computed values of $-[\mathbf{V}\cdot\nabla\phi]$ through its vertical profile and stability in computation. This may be attributed to the fact that a rather strong geopotential gradient exists in the severe storm area which makes its estimate easier. Those area-mean values of energy variables are presented as integral values for the mass of atmosphere between two pressure levels. However, the notation of a vertical integral will be omitted in this paper for the sake of simplicity, although this will be clearly indicated in the physical units used in this presentation. The computation is performed for each individual observation time. Averages during nine single storm periods were obtained as case means. Those case means are then further averaged to obtain the overall average which is simply referred to as the average throughout this paper.

TABLE 1. Kinetic energy balance (W m^{-2}) in the general flow averaged over all nine storm cases within specified layers.

Pressure layer (mb)	$[\partial k/\partial t]$	$-[\nabla\cdot\mathbf{V}k]$	$-[\partial\omega k/\partial p]$	$-[\mathbf{V}\cdot\nabla\phi]$	$[E]$
100–150	−0.30	2.89	−1.59	−2.49	−0.90
150–200	−0.60	−3.67	3.69	6.71	7.33
200–250	0.33	−1.50	2.10	6.95	7.23
250–300	0.43	−0.32	1.05	3.53	3.84
300–350	−0.26	−0.84	1.20	1.11	1.74
350–400	0.14	−0.24	0.14	−0.12	−0.35
400–450	0.31	0.55	−0.30	−0.06	−0.11
450–500	0.00	0.61	−0.81	0.40	0.20
500–550	−0.30	1.70	−1.50	0.31	0.81
550–600	−0.25	1.54	−1.44	0.25	0.60
600–650	−0.13	1.00	−0.99	0.35	0.49
650–700	0.03	−0.10	−0.39	0.45	−0.08
700–750	−0.11	0.06	−0.15	0.66	0.67
750–800	0.14	−0.33	0.23	1.28	1.04
800–850	0.32	−0.01	−0.14	1.91	1.44
850–900	0.49	0.67	−0.59	2.65	2.24
900–968	0.46	0.83	−0.71	4.40	4.08
Total 100–968	0.71	2.85	−0.20	28.31	30.25

4. Balance of kinetic energy in the general flow

The average budget of kinetic energy in the general flow according to Eq. (5) is presented in Table 1. Fig. 3 shows vertical profiles of the generation and dissipation and those of horizontal and vertical transports of kinetic energy.

As discussed by Kung and Smith (1974), it is essential to recognize that the utility of objective energy diagnosis depends very much on the nature of the data input into budget equations. Interpretation of diagnostic results requires careful regard for the scale of processes represented by the data as well as physical implications imposed by computational procedures. The scale of a characteristic circulation pattern in the severe storm area is known to be subsynoptic. The NSSL upper-air observation network area is less than 80,000 km^2. Thus the energy budget of the general flow obtained with the NSSL data may be expected to be subsynoptic in its basic nature, which cannot be observed with the synoptic-scale data. This may be seen from the fact, as we will discuss later in this section (see Tables 3 and 4), that the energy transformations in the severe storm area are strongly influenced by the existence of

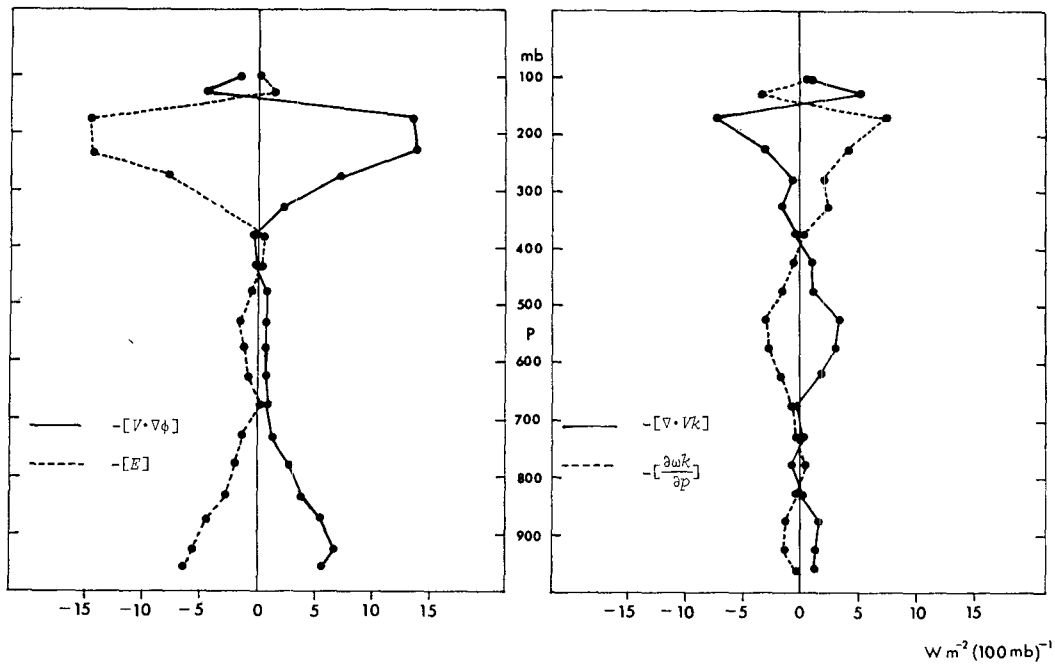

FIG. 3. Average vertical profiles of energy transformations in the general flow.

meso-convective systems in the area. However, it also should be noted that the partial contribution from the larger scales is not filtered out when the NSSL data are applied to Eq. (5). In particular, if the characteristic subsynoptic-scale pattern like severe storms did not exist in the area, the energy budget computed with subsynoptic-scale data might heavily reflect the prevailing synoptic-scale processes. In short, what is meant by "subsynoptic-scale budget" in objective energy diagnosis, should be taken as the energy budget computed with subsynoptic-scale network data.

The vertical profile of the cross-isobaric generation $-[\mathbf{V}\cdot\nabla\phi]$ shows a maximum generation in the planetary boundary layer, a gradual decrease to an insignificant generation in the mid troposphere, and then another maximum generation at the jet stream level. There are significant horizontal inflows of kinetic energy in the mid troposphere as indicated by the positive value of $-[\nabla\cdot\mathbf{V}k]$, and a horizontal outflow in the upper troposphere as indicated by the negative value of the same parameter. Those horizontal outflow and inflow at different layers tend to cancel each other, and thus only contribute 2.85 W m^{-2} to the vertical integral from the surface to 100 mb. The vertical transport of kinetic energy $-[\partial\omega k/\partial p]$ shows divergence in the mid and lower troposphere, and convergence in the upper troposphere. As a result $-[\nabla\cdot\mathbf{V}k]$ and $-[\partial\omega k/\partial p]$ also show cancelling effect at different layers of the atmosphere and the vertical profile of dissipation $[E]$ follows that of generation—*viz.* a maximum in the planetary boundary layer and another at the jet stream level.

The general shape of vertical profiles of the generation $-[\mathbf{V}\cdot\nabla\phi]$ and dissipation $[E]$ in Fig. 3 is very similar to that obtained in the well-developed continental-size cyclone by Kung (1966). The magnitude of the values of generation and dissipation, 28.3 W m^{-2} for $-[\mathbf{V}\cdot\nabla\phi]$ and 30.2 W m^{-2} for $[E]$ from the surface to 100 mb, is comparable with 16.2 to 27.4 W m^{-2} for major synoptic-scale cyclones in the mature stage as compiled from various studies by Kung and Smith (1974). The energetics role of mature intense cyclones is still under investigation. Works on energy conversion within a cyclone have been done in various case studies (e.g., White and Saltzman, 1956; Eddy, 1965) in terms of the correlation between the vertical motion and temperature fields. However, as discussed by Kung and Smith (1974), Newell *et al.* (1970) and Newton (1970), the processes involved between the conversion and cross-isobaric generation is a particularly important linkage to be investigated in the future. Kung's (1966) study with well-developed cyclone systems during 15–24 January 1963 over North America shows that the cyclone has generated 25.8 W m^{-2} and exported 20.5 W m^{-2} of kinetic energy, whereas various case studies suggest (see Kung and Smith, 1974) that it also may consume kinetic energy imported into the area under certain conditions. The area of subsynoptic-scale storms, *viz.* the storm environment, in this study has on the average consumed some kinetic energy imported from the surroundings. However, the amount of imported kinetic energy is rather insignificant as indicated by the average vertical total 2.9 W m^{-2} of $-[\nabla\cdot\mathbf{V}k]$ (see Table 1), which is only 9% of 30.3 W m^{-2}

of the dissipation in the area. This may suggest that the subsynoptic-scale storm environment is nearly adequately supported by the internal supply of kinetic energy during the observation period. However, the energy budget presented here is strictly for the overall average, and should be interpreted as the general effect in the storm area.

The terms $[E]$ and $[E^*]$ which are obtained as residual terms to balance Eqs. (5) and (8) are customarily and conveniently regarded as the dissipation. However, much controversy has developed around these terms as they represent very important, yet difficult processes to estimate as well as to interpret (Ellsaesser, 1969; Kung, 1969, 1975; Lorenz, 1967; Smith, 1973; Wiin-Nielsen, 1968). As discussed by Kung and Smith (1974), these terms conceptually represent the eventual thermodynamic irreversible dissipation process by friction. In the numerical models it can be formulated so that it represents or parameterizes the energy cascading or frictional processes supposedly taking place. In the observational studies with upper-air data, however, there is no guarantee that $[E]$ or $[E^*]$ obtained as a residual term represents frictional processes in the true thermodynamic sense. It is important to recognize here that this is for the most part the sink or disappearance of kinetic energy from the observed scale, which should be the net input into various scales that cannot be explicitly computed with upper-air data of the given network. If $[E]$ or $[E^*]$ gives a negative value, it should mean energy input from other scales to observed scales of motion instead of energy sink.

The foregoing discussion is particularly applicable to dissipation values obtained in the free atmosphere whereas those in the planetary boundary layer may be closely identified with friction at the boundary. By taking $[E]$ in the 900–968 mb layer in Table 1 as the boundary layer dissipation, 4.08 W m^{-2} is about twice the boundary layer dissipation that may be expected in the area without severe storms (Kung, 1966). Though not listed in the table, it will be pertinent here to note that the boundary layer dissipation we computed reached around 10 W m^{-2} at certain synoptic observations of the network, indicating the maximum frictional dissipation the boundary layer may perform in a storm environment. The dissipation sink $[E]$ in the free atmosphere above the 900 mb level, as shown in Table 1, is 26.17 W m^{-2} which is 86% of the total average dissipation of 30.25 W m^{-2}.

Table 2 lists the average kinetic energy generation during each of 9 storm cases. A wide range of the magnitude of $-[\mathbf{V}\cdot\nabla\phi]$ among those case averages is readily observed. Although the majority of cases show the general bimodal shape of the vertical distribution of $-[\mathbf{V}\cdot\nabla\phi]$, a few cases are obvious departures from this. The departures should be explained according to the fact that the observation was initiated when the storm had approached the network area and terminated when the storm had left the area. The initiation and termination of the observation period were thus by no means adjusted to correspond with the life cycle of the thunderstorm or squall line.

Examination of the radar photographs (see McInnis, 1970) and computed fields of vertical motion indicate that the cases of 4/22/66, 5/20/67, 5/30/67, 6/10/67 are those in which active convective cells were identified in the area and strong vertical motion prevailed. In those cases, as shown in Table 2, the magnitude of kinetic energy generation is very large, particularly at the jet-stream level. The case of 6/08/66 belongs to this category, too, but the process is less intense. In the cases of 5/20/66, 5/31/66, 5/28/67 and 6/08/67, con-

TABLE 2. Kinetic energy generation $-[\mathbf{V}\cdot\nabla\phi]$ (W m^{-2}) averaged in each storm case within specified layers.

	Case								
	4/22/66	5/20/66	5/31/66	6/08/66	5/20/67	5/28/67	5/30/67	6/08/67	6/10/67
Pressure layer	Number of synoptic observation times								
(mb)	5	7	4	8	4	5	7	3	5
100–150	−3.42	−12.95	−11.73	−0.96	1.75	−0.79	4.70	−2.25	3.21
150–200	37.15	− 9.99	− 7.57	1.87	17.65	0.24	22.35	−2.48	1.20
200–250	29.95	− 5.19	− 4.72	2.85	16.21	−0.20	28.17	−2.78	−1.71
250–300	13.14	− 3.58	− 3.71	1.42	8.94	0.15	11.61	−4.67	8.51
300–350	6.67	− 3.38	− 2.82	−1.25	4.67	0.04	2.57	−5.47	8.97
350–400	2.72	− 2.93	− 2.61	−1.90	1.43	−0.48	−1.45	−6.00	10.18
400–450	1.10	− 2.29	− 2.11	−1.03	0.43	−1.01	0.94	−5.98	9.42
450–500	1.77	− 2.12	− 1.92	−1.18	1.29	−0.54	3.29	−4.17	7.21
500–550	2.16	− 1.56	− 2.18	−0.61	1.59	−0.53	3.22	−2.68	3.36
550–600	1.43	− 1.32	− 1.91	1.10	2.12	0.05	0.81	−2.11	2.11
600–650	0.15	− 0.96	− 1.31	2.70	1.90	0.39	1.42	−2.58	1.45
650–700	1.68	− 0.14	− 0.63	3.08	1.29	0.59	0.82	−3.79	1.16
700–750	3.15	0.75	− 0.18	2.71	1.13	0.79	−0.14	−2.92	0.66
750–800	4.32	1.97	0.11	2.26	1.17	1.16	0.16	−1.68	2.01
800–850	3.74	3.14	0.16	2.65	0.61	1.52	1.47	0.02	3.87
850–900	2.65	3.96	0.52	3.25	0.38	1.35	2.46	3.42	5.84
900–968	1.49	5.16	1.69	4.30	7.23	2.47	2.78	7.03	7.46
Total 100–968	109.85	−31.42	−40.94	21.25	69.81	5.21	85.19	−39.10	74.91

TABLE 3. Kinetic energy balance (W m^{-2}) in the general flow during the 5/30/67 storm case averaged over seven synoptic observation times within specified layers.

Pressure layer (mb)	$[\partial k/\partial t]$	$-[\nabla\cdot\mathbf{V}k]$	$-[\partial\omega k/\partial p]$	$-[\mathbf{V}\cdot\nabla\phi]$	$[E]$
100–150	−0.29	−0.66	3.23	4.70	7.56
150–200	7.83	−10.80	11.79	22.35	15.50
200–250	5.46	−14.82	4.57	28.17	12.46
250–300	3.91	−5.60	1.23	11.61	3.33
300–350	1.40	0.35	0.42	2.57	1.95
350–400	0.98	5.61	−0.68	−1.45	2.50
400–450	0.80	10.25	−3.04	0.94	7.35
450–500	0.51	9.46	−6.57	3.29	5.67
500–550	0.89	8.07	−5.59	3.22	4.81
550–600	0.57	6.50	−5.24	0.81	1.49
600–650	0.93	5.10	−1.81	1.42	3.78
650–700	1.20	3.05	−0.19	0.82	2.47
700–750	0.44	1.44	0.24	−0.14	1.10
750–800	−0.07	0.17	0.61	0.16	1.02
800–850	−0.66	−0.59	0.30	1.47	1.83
850–900	−0.05	−1.22	0.35	2.46	1.64
900–968	0.38	−1.36	0.52	2.78	1.57
Total 100–968	24.23	14.95	0.13	85.19	76.04

vective activity was either little noted, failed to develop, or was weak; the field of vertical motion was either variable or weak downward. These cases are characterized by the adiabatic destruction of kinetic energy (negative $-[\mathbf{V}\cdot\nabla\phi]$ values) in the upper troposphere. Clearly the subsynoptic-scale energy transformation is related to the meso-convective systems existing in the area and/or stages of the storm development.

Case averages of kinetic energy budget for 5/30/67 and 6/08/66 are shown in Tables 3 and 4 to contrast the kinetic energy balance in the severe storm environments with and without active convective cells identified in the area. These cases are chosen for illustration since they represent typical contrasting situations in the area and both have had rather long, continuous records of seven synoptic observations during the periods. With the existence of a strong meso-convective system in the area (Table 3), the cross-isobaric generation $-[\mathbf{V}\cdot\nabla\phi]$ at the jet stream level is very strong. A strong horizontal outflow of kinetic energy at that level and inflow below that level are significant. The inflow of kinetic energy in the mid troposphere is clearly related with the significant net vertical transport of kinetic energy from the mid troposphere to the jet stream level as indicated by the vertical profile of $-[\partial\omega k/\partial p]$. As a result, the dissipation term shows a prime maximum of the kinetic energy sink at the jet stream level and the secondary maximum of the sink in the mid troposphere. Interestingly, the boundary layer dissipation in the 900–968 mb layer due to the surface friction is not dominant. Indication is that this is the case when the free atmosphere is energetically active at this scale with the existence of meso-convective systems in the area.

When active convective systems are not present in the area (Table 4), a different situation is observed. Above the lower troposphere, a general adiabatic destruction of kinetic energy is observed as indicated by negative values of $-[\mathbf{V}\cdot\nabla\phi]$. The horizontal outflow of kinetic energy is indicated in most parts of the atmosphere, and the vertical transport term is not significant. This leaves the $[E]$ value negative in the mid and upper layers, indicating required energy input from other scales to the subsynoptic-scale processes under the condition.

As the magnitude of the energy parameters shown in Table 3 is much larger than that in Table 4, the averages of those two contrasting situations actually become qualitatively similar to what is shown in Table 1 as the overall case averages. As indicated in our previous studies (McInnis, 1970; McInnis and Kung, 1972), each term of the budget equation also oscillates in a wide range during the storm period or the passage of the storm. These indicate the complicated pattern of energy transformation in the severe storm area. Thus for the detailed energetics information throughout a formation and decay of subsynoptic-scale storms as well as throughout the storm area, it is necessary to have comprehensive, continuous synoptic descriptions of the fields of motion in synoptic and subsynoptic scales in relation to existing mesosystems identifiable in the storm area.

The energy budget computations presented previously by McInnis and Kung (1972) were necessarily crude since most of the refined techniques of numerical analysis with the subsynoptic-scale upper-air network as employed in this study had not then been developed. In particular, the vertical motion ω was substituted by an area-mean $[\omega]$; fields of meteorological variables were analyzed at balloon position without any degree of optimization; and the scheme lacked any smoothing of

TABLE 4. Kinetic energy balance (W m^{-2}) in the general flow during the 5/20/66 storm case averaged over seven synoptic observation times within specified layers.

Pressure layer (mb)	$[\partial k/\partial t]$	$-[\nabla\cdot\mathbf{V}k]$	$-[\partial\omega k/\partial p]$	$-[\mathbf{V}\cdot\nabla\phi]$	$[E]$
100–150	−3.40	−3.51	−0.48	−12.95	−13.55
150–200	−6.46	−6.98	−0.98	−9.99	−11.48
200–250	−3.04	−2.74	0.04	−5.19	−4.85
250–300	−2.26	−0.71	0.28	−3.58	−1.75
300–350	−0.97	0.06	−0.47	−3.38	−2.82
350–400	0.16	−0.18	0.09	−2.93	−3.18
400–450	−0.09	−0.77	0.24	−2.29	−2.72
450–500	−0.13	−0.93	0.51	−2.12	−2.40
500–550	−0.19	−0.06	0.31	−1.56	−1.13
550–600	−0.52	0.01	0.12	−1.32	−0.68
600–650	−0.58	−0.14	0.01	−0.96	−0.52
650–700	−0.57	−0.07	0.18	−0.14	0.54
700–750	−0.47	0.06	−0.17	0.75	1.10
750–800	−0.23	−0.65	0.19	1.97	1.74
800–850	0.28	−0.88	0.14	3.14	2.12
850–900	1.35	−1.18	0.18	3.96	1.61
900–968	1.97	0.20	−0.15	5.16	3.25
Total 100–968	−15.15	−18.47	0.03	−31.42	−34.71

TABLE 5. Comparison of $[k]$ and $[k_e]$ within specified layers.

Pressure layer (mb)	$[k]$ (10^5 J m^{-2})	$[k_e]$ (10^5 J m^{-2})	$[k_e]/[k]$ (%)
100–150	1.28	0.03	2.3
150–200	2.24	0.05	2.2
200–250	1.64	0.05	3.0
250–300	1.20	0.04	3.3
300–350	1.03	0.03	2.9
350–400	0.92	0.02	2.2
400–450	0.82	0.03	3.7
450–500	0.73	0.02	2.7
500–550	0.65	0.03	4.6
550–600	0.58	0.03	5.2
600–650	0.51	0.02	3.9
650–700	0.42	0.02	4.8
700–750	0.35	0.02	5.7
750–800	0.32	0.02	6.3
800–850	0.34	0.02	5.9
850–900	0.35	0.04	11.4
900–968	0.37	0.04	10.8
Total 100–968	13.76	0.51	3.7

TABLE 6. Kinetic energy balance (W m^{-2}) in disturbances averaged over all nine storm cases within specified layers.

Pressure layer (mb)	$[\partial k_e/\partial t]$	$-[\nabla\cdot\mathbf{V}k_e]$	$-[\partial\omega k_e/\partial p]$	C	$-[\mathbf{V}^*\cdot\nabla\phi^*]$	$[E^*]$
100–150	−0.02	−0.07	−0.04	−0.07	−0.16	−0.32
150–200	0.11	−0.32	0.13	−0.04	−0.57	−0.91
200–250	0.10	−0.44	0.11	0.05	−0.41	−0.79
250–300	0.04	−0.18	−0.03	0.03	−0.14	−0.37
300–350	−0.02	−0.03	0.02	0.04	−0.02	0.01
350–400	0.04	0.03	0.00	−0.01	−0.03	−0.05
400–450	−0.02	0.07	0.03	−0.04	−0.01	0.07
450–500	0.00	0.07	−0.06	−0.04	0.04	0.01
500–550	0.02	0.15	−0.03	−0.03	0.07	0.15
550–600	0.00	0.14	−0.07	−0.01	0.10	0.17
600–650	0.04	0.07	−0.07	−0.01	0.26	0.21
650–700	0.06	−0.02	0.01	−0.02	0.14	0.05
700–750	0.01	0.03	0.02	−0.01	0.09	0.13
750–800	0.03	0.01	0.03	−0.01	0.09	0.10
800–850	0.02	0.03	0.08	−0.05	0.20	0.24
850–900	0.02	0.09	−0.01	−0.05	0.43	0.43
900–968	−0.11	0.20	−0.13	−0.10	0.61	0.69
Total 100–968	0.33	−0.19	0.00	−0.37	0.70	−0.18

the computed fields required for the subsynoptic-scale data. However, comparison of the average energy budgets in this study and in that of McInnis and Kung indicate that there is a qualitative agreement between them, and tentative conclusions by McInnis and Kung may be sustained.

5. Energy transformations in disturbances

The budget equations as formulated in (8) and (10) permit the description of the energetics properties of transient, evolving disturbances in the space domain which may be present at any given observation time in the network area. Kung and Merritt (1974) and Kung (1975) have shown that with the large-scale upper-air network data over the western tropical Pacific those equations may describe energy transformations in the well-recognized tropical wave disturbances.

In the middle-latitude area where subsynoptic-scale storm systems dominate, i.e., near, or in the area of squall lines and thunderstorms, the atmospheric flow pattern and fields of meteorological parameters are known to be influenced by the existence of mesosystems and also by the passage of the meso- and subsynoptic-scale waves in the area. Using the data from the 5/28/67 NSSL case Fankhauser (1969) depicted the disturbances observable in the area and the transient nature of those disturbances through the presentation of hourly patterns. Alberty and Van Sickle (1969) used the same 5/28/67 data and Coleman (1969) used the 5/30/67 data to detect the existence of mesoscale internal-gravity waves in the area with a wavelength of 150 km and a period of 3 h. The importance of subsynoptic-scale waves with wavelengths of 1000 km in cyclone areas has been discussed by Nitta and Yamamoto (1973); the passage or modification of such waves is also expected to influence the flow pattern in the subsynoptic-scale network area.

Those systems of disturbances with a range from meso to subsynoptic scale impose transient disturbances on the flow pattern which are observed with the subsynoptic-scale network. Although details of those transient disturbances are not yet well known, their basic energetics properties can be observed to a certain degree by applying Eqs. (8) and (10) to the NSSL data to provide insight into the nature of those disturbances.

As shown in Table 5, the eddy kinetic energy due to those disturbances is about 3.7% of the total kinetic energy in the general flow. The percentage ratio of eddy kinetic energy in the total kinetic energy is highest with more than 10% in the lower troposphere; it decreases upward to 2–3% in the upper part of the atmosphere. However, it should be noted that, despite

TABLE 7. Sources for kinetic energy generation (W m^{-2}) in disturbances averaged over all nine storm cases within specified layers.

Pressure layers (mb)	$-[\mathbf{V}^*\cdot\nabla\phi^*]$	$-[\omega^*\alpha^*]$	$-[\nabla\cdot\mathbf{V}^*\phi^*]$	$-[\partial\omega^*\phi^*/\partial p]$
100–150	−0.16	0.03	−0.10	−0.09
150–200	−0.57	0.02	0.18	−0.76
200–250	−0.41	−0.18	0.11	−0.34
250–300	−0.14	−0.12	0.02	−0.04
300–350	−0.02	−0.08	−0.13	0.19
350–400	−0.03	−0.01	−0.10	0.08
400–450	−0.01	0.01	−0.10	0.08
450–500	0.04	−0.01	−0.06	0.11
500–550	0.07	0.04	−0.03	0.06
550–600	0.10	0.03	0.02	0.06
600–650	0.26	0.01	−0.02	0.27
650–700	0.14	0.04	−0.02	0.13
700–750	0.09	0.04	0.04	0.01
750–800	0.09	0.12	0.11	−0.14
800–850	0.20	0.17	0.12	−0.09
850–900	0.43	0.19	0.08	0.16
900–968	0.61	0.14	0.03	0.44
Total 100–968	0.70	0.44	0.15	0.11

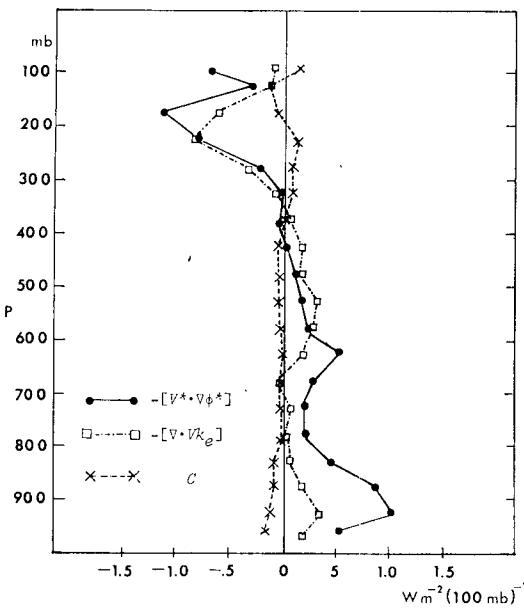

FIG. 4. Average vertical profiles of internal and external sources of eddy kinetic energy in disturbances.

the relatively small magnitude of k_e in the upper part of the atmosphere due to the increasing k, the value of k_e shows its maximum in the upper troposphere. As indicated in the analysis by Kung and Behrens (1974), the subsynoptic-scale range links the kinetic energy flow between larger and smaller scales of motion. Thus, it is interesting to examine the kinetic energy in disturbances observed in the subsynoptic-scale flow, though the scale interactions of energy may not necessarily appear appreciably in disturbances of fields of horizontal motion.

The vertical distribution of the overall budget of kinetic energy balance in disturbances, according to Eq. (8), is shown in Table 6. The component sources in relation with the eddy generation as formulated in Eq. (10) are further presented in Table 7. The eddy generation $-[\mathbf{V}^*\cdot\nabla\phi^*]$ shows a maximum in the lower troposphere and gradually decreases to a small value in the mid-troposphere. Unlike the generation $-[\mathbf{V}\cdot\nabla\phi]$ in the general flow, $-[\mathbf{V}^*\cdot\nabla\phi^*]$ further decreases to the negative maximum at the jet stream level where $-[\mathbf{V}\cdot\nabla\phi]$ is maximum, although $-[\mathbf{V}^*\cdot\nabla\phi^*]$ is the component of eddy contribution in $-[\mathbf{V}\cdot\nabla\phi]$.

The term C defined in Eq. (9) shows that the eddies give up kinetic energy to the basic flow as defined by the area-mean components of the general flow, except that eddy disturbances draw kinetic energy from the area-mean flow at the jet stream level where the negative eddy generation is maximum. The vertical transport term $-[\partial\omega k_e/\partial p]$ shows some convergence of eddy kinetic energy above the planetary boundary layer and in the upper troposphere. The horizontal transport term $-[\nabla\cdot Vk_e]$ shows a general convergence of eddy kinetic energy in the mid and lower troposphere and divergence in the upper troposphere, with the vertically integrated value of -0.19 W m^{-2} of exported k_e out of the area only half the conversion C from the eddy to area-mean flow. Fig. 4 contrasts their vertical profiles. It appears that the mid and lower troposphere are the major source regions of eddy kinetic energy and the upper troposphere is the sink region.

The value of eddy dissipation $[E^*]$ shown in Table 6 is maximum in the lower atmosphere, and the frictional dissipation in the planetary boundary layer may be readily inferred by this as well as by the lower boundary maximum of $[E]$ in the general flow (Table 1). The value of $[E^*]$ decreases upward and becomes negative in the upper troposphere and above. This is in sharp contrast to the overall average values of $[E]$ in the general flow that shows the primary dissipation at the jet stream level. The maximum dissipative sink in the upper troposphere as shown by $[E]$ could imply a number of possible frictional effects or transfer mechanisms in the upper troposphere (e.g., Lilly, 1972; Panofsky, 1969). However, any direct frictional effect may not provide adequate explanation for $[E^*]$ in disturbances of the upper troposphere which shows a significant negative value. The negative eddy dissipation should represent the residual effects over all related scales which cannot be explicitly observed at the scale of the given observational network. It implies that these negative $[E^*]$ values indicate the energy input from other scales of process, larger or smaller, to observed scales of disturbances. In the upper troposphere as illustrated in Fig. 5, the eddies adiabatically destroy the kinetic energy as indicated by negative

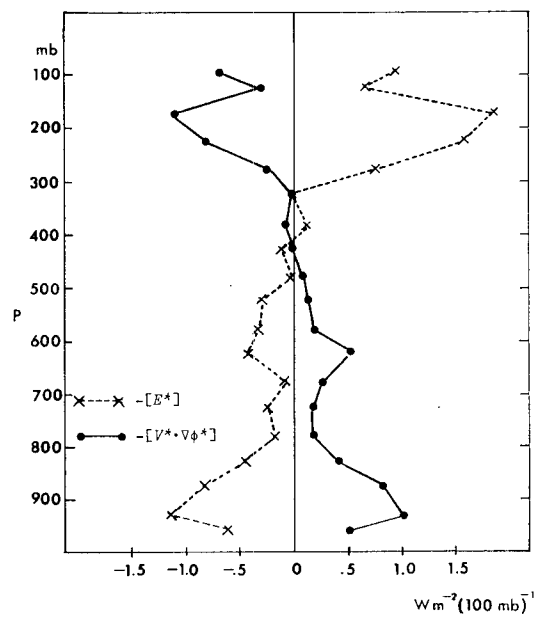

FIG. 5. Comparison of eddy kinetic energy generation and dissipation in disturbances.

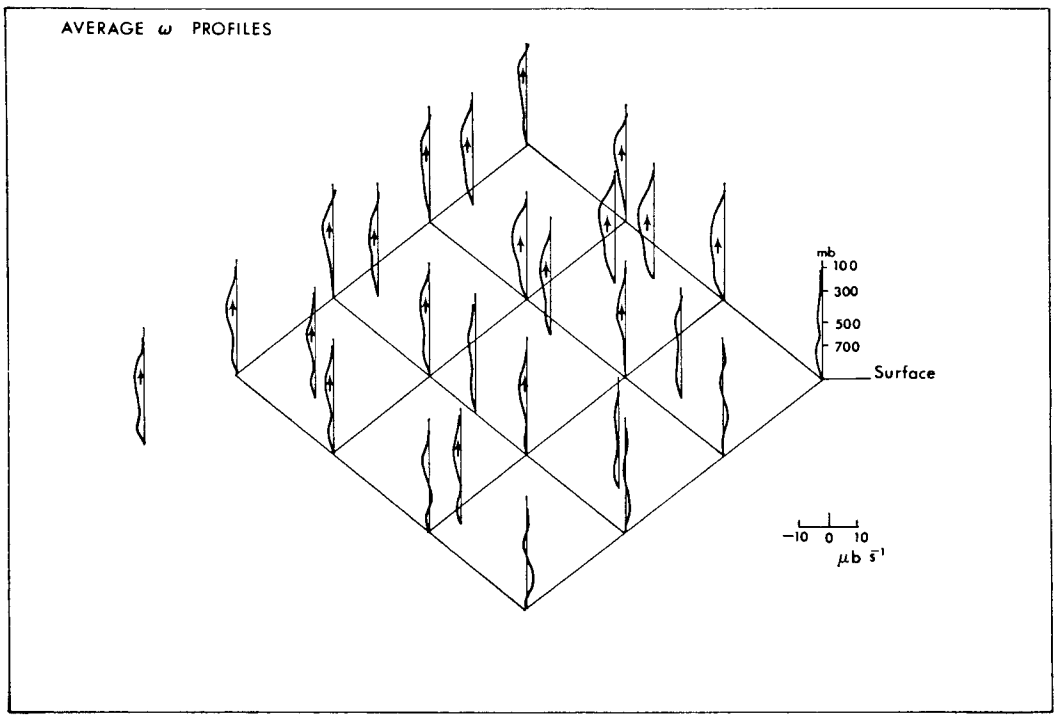

FIG. 6. Distribution of average ω profiles at observation stations and analysis grids.

values of $-[\mathbf{V}^*\cdot\nabla\phi^*]$, but other explicitly observed terms of eddy kinetic energy (Table 6 and Fig. 4) either give negative values as well, or are too small to make up the negative $-[\mathbf{V}^*\cdot\nabla\phi^*]$. Thus other scales of processes must make up the deficit to maintain the disturbances in the upper troposphere. This is consistent with Kung and Behrens' (1974) study that the flow of kinetic energy betweeen large and small scales through the subsynoptic scales could be observed in the upper troposphere.

Table 7 presents component source terms of kinetic energy in relation to the eddy generation $-[\mathbf{V}^*\cdot\nabla\phi^*]$. The baroclinic conversion $-[\omega^*\alpha^*]$ shows a major source in the lower troposphere and negative conversion in the upper troposphere. The horizontal convergence of eddy potential energy $-[\nabla\cdot\mathbf{V}^*\phi^*]$ gives significant energy source in the lower and upper troposphere, but this term shows a net export of eddy potential energy in the mid-troposphere. As shown in Fig. 6, the general field of the vertical motion is upward. However, as shown by values of $-[\partial\omega^*\phi^*/\partial p]$ in Table 7, the upper troposphere supplies eddy potential energy to the lower part of the troposphere through vertical eddy coupling. From the vertical integrals of those values, we see that local baroclinic conversion $-[\omega^*\alpha^*]$ accounts for 63% of the eddy generation $-[\mathbf{V}^*\cdot\nabla\phi^*]$ from the surface to the 100 mb level. The supply of eddy potential energy from the surrounding as indicated by $-[\nabla\cdot\mathbf{V}^*\phi^*]$ only accounts for 21% of the eddy generation.

6. Summary and conclusions

This is an attempt to observe the kinetic energy balance under severe storm conditions with a subsynoptic-scale upper-air network. The optimized analysis scheme devised by Kung (1972, 1973) for kinematic computation of the vertical motion field and other meteorological fields has been modified and applied to the NSSL subsynoptic-scale network data during 1966 and 1967 storm periods.

On the average, the import of kinetic energy is rather negligible, and most of the kinetic energy consumed in the storm area is generated within the area. The general shape of vertical profiles of the generation $-[\mathbf{V}\cdot\nabla\phi]$ and dissipation $[E]$ is very similar to that in well-developed major cyclones with maxima in the planetary boundary layer and at the jet stream level. The average magnitude of the energy transformation is also comparable with what is observed in major synoptic-scale cyclones. However, comparison of energy budget during different storm periods reveals that the magnitude of subsynoptic-scale energy transformation may vary widely depending upon the existence and strength of meso-convective systems in the area. With active convective cells in the area, the generation and dissipation of kinetic energy in the upper troposphere are very large; with little noted convective activity, there may be a significant destruction of kinetic energy by the cross-isobaric flow in the upper troposphere.

Transient disturbances in the storm area may be detected with the subsynoptic-scale upper-air network. The balance of eddy kinetic energy observed with the NSSL data shows some interesting energetics features in relation to those disturbances. The cross-isobaric generation term $-[\mathbf{V}^* \cdot \nabla\phi^*]$ has a positive maximum in the lower troposphere, but indicates adiabatic destruction of eddy kinetic energy in the upper troposphere. The eddies also give up kinetic energy to the basic flow which is defined by the area-mean component of the flow. Examination of terms in the eddy kinetic energy equation indicates that the mid and lower troposphere is the major source region of eddy kinetic energy and the upper troposphere is the sink region through the cross-isobaric generation. The eddy dissipation obtained as the residual term of the eddy kinetic energy equation shows negative values in the upper troposphere, which is in sharp contrast to the dissipation of the general flow with its primary maximum in the upper troposphere. The negative eddy dissipation would indicate the energy input from other scales of process to observed scale of disturbances.

Component source terms of eddy potential energy in relation to eddy generation of kinetic energy have also been examined. Of the three source terms, the baroclinic conversion $-[\omega^*\alpha^*]$ appears to be the major source of eddy kinetic energy in those disturbances.

Acknowledgment. Technical assistance by S. A. McConnell, A. J. Siegel, D. L. Kliethermes and P. P. Lux, and reading of the original manuscript by H. A. Burgdorf are sincerely acknowledged.

REFERENCES

Alberty, R. L. and K. L. Van Sickle, 1969: An analysis of a severe local storm using isentropic trajectories. U. S. Naval Postgraduate School, NPS-51A 19081A, 135 pp. (Available from NTIS—AD 693046.)

Behrens, J. B., 1972: An analysis of sub-grid scale turbulent energy. M.S. thesis, University of Missouri-Columbia, 69 pp.

Coleman, R. J., 1969: A diagnostic analysis of the 30 May 1967 squall line in Central Oklahoma. M. S. thesis, U. S. Naval Postgraduate School 142 pp. (Available from NTIS—AD 706014.)

Eddy, A., 1965: Kinetic energy production in a mid-latitude storm. *J. Appl. Meteor.*, **4**, 569–575.

Ellsaesser, H. W., 1969: A climatology of epsilon (atmospheric dissipation). *Mon. Wea. Rev.*, **97**, 415–423.

Fankhauser, J. C., 1969: Convective processes resolved by a mesoscale rawinsonde network. *J. Appl. Meteor.*, **8**, 778–798.

Kung, E. C., 1966: Kinetic energy generation and dissipation in the large-scale atmospheric circulation. *Mon. Wea. Rev.*, **94**, 67–82.

——, 1969: Further study on the kinetic energy balance. *Mon. Wea. Rev.*, **97**, 573–581.

——, 1972: A scheme for kinematic estimate of large-scale vertical motion with an upper-air network. *Quart. J. Roy. Meteor. Soc.*, **98**, 402–411.

——, 1973: Note on design of an optimized computation scheme for kinematic vertical motion field. *Mon. Wea. Rev.*, **101**, 685–690.

——, 1975: Balance of kinetic energy in the tropical circulation over the western Pacific. *Quart. J. Roy. Meteor. Soc.* (in press).

—— and J. B. Behrens, 1974: An analysis of subsynoptic scale turbulent energy with upper-air wind profiles. *J. Meteor. Soc. Japan*, **52**, 218–229.

——, and L. P. Merritt, 1974: Kinetic energy sources in large-scale tropical disturbances over the Marshall Islands area. *Mon. Wea. Rev.*, **102**, 489–502.

——, and P. J. Smith, 1974: Problems of large-scale kinetic energy balance—a diagnostic analysis in GARP. *Bull. Amer. Meteor. Soc.*, **55**, 768–777.

Lilly, D. K., 1972: Wave momentum flux—a GARP problem. *Bull. Amer. Meteor. Soc.*, **53**, 17–23.

Lorenz, E. N., 1967: *The Nature and Theory of the General Circulation of the Atmosphere.* World Meteorological Organization, 161 pp.

McInnis, D. H., 1970: A meso-scale energy analysis of atmospheric motion. Ph.D. thesis, University of Missouri-Columbia, 143 pp.

——, and E. C. Kung, 1972: A study of sub-synoptic scale energy transformations. *Mon. Wea. Rev.*, **100**, 126–132.

Newell, R. E., D. G. Vincent, T. G. Dopplick, D. Ferruzza and J. W. Kidson, 1970: The energy balance of the global atmosphere. *Global Circulation of the Atmosphere*, G. A. Corby, Ed., Roy. Meteor. Soc., 42–90.

Newton, C. W., 1970: The role of extratropical disturbances in the global atmosphere. *Global Circulation of the Atmosphere*, G. A. Corby, Ed., Roy. Meteor. Soc., 137–158.

Nitta, T., and J. Yamamoto, 1973: A diagnosis of the formation of intermediate-scale disturbances near Japan, the western Pacific, and southeast Asia. *Papers Meteor. Geophy.*, **24**, 289–309.

O'Brien, J. J., 1970: Alternative solutions to the classical vertical velocity problem. *J. Appl. Meteor.*, **8**, 197–203.

Panofsky, H. A., 1969: Internal atmospheric turbulence. *Bull. Amer. Meteor. Soc.*, **50**, 539–543.

Smith, P. J., 1973: Midlatitude synoptic scale systems: Their kinetic energy budgets and role in the general circulation. *Mon. Wea. Rev.*, **101**, 757–762.

Stidd, C. K., 1967: The use of eigenvectors for climatic estimates. *J. Appl. Meteor.*, **6**, 255–264.

White, R. M., and B. Saltzman, 1956: On the conversion between potential and kinetic energy in the atmosphere. *Tellus*, **8**, 357–363.

Wiin-Nielsen, A., 1968: On the intensity of the general circulation of the atmosphere. *Rev. Geophys.*, **6**, 559–579.

Wrigley, C. L., 1973: Isolation of turbulent kinetic energy in upper-air profiles. M.S. thesis, University of Missouri-Columbia, 40 pp.